

## Scaling of the Excess Energy in Thermodynamically Unstable Solutions

R. Toral and J. Marro

*Departament de Física Teòrica, Universitat de Barcelona, Barcelona 08028, Spain*

(Received 18 July 1984)

The excess energy or enthalpy in thermodynamically unstable solutions relaxing towards equilibrium is related to properties of the cluster distribution. We thus infer a general scaling *Ansatz* and the simultaneous occurrence of two mechanisms during the system evolution, both in agreement with data. We also find two different classes of phase points, and propose a graphical method to analyze these matters in microcalorimetric measurements.

PACS numbers: 64.60.Cn, 05.20.-y, 81.30.Mh

Many homogeneous binary mixtures suddenly brought into a two-phase region may become thermodynamically unstable thus undergoing phase separation. The kinetics of these processes can be analyzed in some cases by monitoring the structure function  $S(\mathbf{k}, t)$ , where  $\mathbf{k}$  is a wave vector and  $t$  the time since quenching.<sup>1</sup>  $S(\mathbf{k}, t)$  reflects, in a way which is not quite understood yet, the behavior of the cluster or droplet distribution,  $n_l(t)$ , with the cluster size  $l$  and with  $t$  while phase separation occurs. When the mean cluster radius or some other characteristic length  $R(t)$  becomes well defined, say when  $T \ll T_c$ , so that the correlation length is rather irrelevant, and  $t > t_s$  (a transient time which is a function of  $T$  and composition), universal features are observed during the system relaxation.<sup>1-3</sup> Namely,  $S(k, t) = R(t)^3 F(kR(t))$ , where  $F$  is a rather universal function.<sup>3</sup> Whereas this scaling behavior has attracted some theoretical attention,<sup>1-5</sup> more work needs to be done in order to clarify the range of validity of both the scaling of  $S$  with time and the universality of  $F$  and to generalize these properties to physical quantities other than the structure function. In this Letter we relate the structure function, cluster distribution, and system excess energy, make some specific predictions concerning scaling and universality which seem well confirmed by experimental data, and give a simple graphical method to analyze microcalorimetric measurements and computer-generated data. We also infer the simultaneous presence of two different mechanisms during the system evolution and its significance.

For the sake of simplicity we shall refer here to the lattice-gas model system with a Kawasaki stochastic hopping dynamics<sup>1</sup> where the  $N (= L^3)$  sites of a simple cubic lattice with periodic boundary conditions, at positions  $\mathbf{r}_i$ ,  $i = 1, \dots, N$ , hold occupation variables  $\eta(\mathbf{r}_i) = +1, -1$  according to whether there is a particle or a hole at site  $i$ . The number of particles,  $\rho N = (1 - \bar{\eta})N/2$ ,  $\bar{\eta}N = \sum_i \eta(\mathbf{r}_i)$ , remains constant

during the system evolution. The system configurational energy is defined as

$$E(t) = -\frac{1}{2} \sum_{i,j} J_{ij} \eta(\mathbf{r}_i, t) \eta(\mathbf{r}_j, t).$$

Here  $J_{ij} > 0$  so that it represents a "ferromagnetic" interaction leading to decomposition below  $T_c$  into a *liquid phase* ("large" clusters, say  $l > l_c$ ) surrounded by a *gas phase* (monomers, dimers, etc. up to  $l \leq l_c$ ).

The structure function can be related to the energy via an equation which was essentially written before by Binder<sup>5</sup>:

$$E(t) = -\frac{1}{2} [ \sum_{\mathbf{k}} \tilde{J}(\mathbf{k}) S(\mathbf{k}, t) + N \bar{\eta} \tilde{J}(0) ]. \quad (1)$$

Here

$$\tilde{J}(\mathbf{k}) = \sum_i J_{ij} \exp[i\mathbf{k} \cdot (\mathbf{r}_i - \mathbf{r}_j)].$$

The simplest interaction corresponds to  $J_{ij} = J$  when  $i$  and  $j$  are nearest neighbors and  $J_{ij} = 0$  otherwise; it then follows that

$$j(\mathbf{k}) \equiv J(\mathbf{k})/2J = \cos k_x + \cos k_y + \cos k_z, \quad j(0) = 3,$$

and the excess energy  $\Delta E(t) \equiv E(t) - E(\infty)$  can be written as

$$\begin{aligned} \Delta E(t)/JN \\ = -(\bar{\eta}_c^2 - \bar{\eta}^2) [ N^{-1} \sum_{\mathbf{k}} j(\mathbf{k}) S_1(\mathbf{k}, t) - 3 ], \end{aligned} \quad (2)$$

where  $\bar{\eta}_c$  is the value of  $\bar{\eta}$  at the coexistence line,

$$S_1(\mathbf{k}, t) = [S(\mathbf{k}, t) - S_c(\mathbf{k}, T)] (\bar{\eta}_c^2 - \eta^2)^{-1},$$

with  $S_c(\mathbf{k}, T)$  the equilibrium structure function at the coexistence line and  $S_1(\mathbf{k}, \infty) = N \delta(\mathbf{k})$ , a Dirac delta function, for a macroscopic system. Note that  $S_1(k, t)$  aims to represent that part of the structure function which corresponds to the liquid phase. Now we may use spherical averages in (2); assuming isotropic conditions and replacing the sum by an integral we have

$$\sum_{\mathbf{k}} j(\mathbf{k}) S_1(\mathbf{k}, t) = \int_0^\kappa (L/2\pi)^3 (\pi/2) k^2 dk j(k) S_1(k, t), \quad (3)$$

where the cutoff is  $\kappa \approx 2\pi$ . Here  $j(k) = 3k^{-1} \sin k$  for  $0 \leq k \leq 2\pi$ , and a rather complicated expression for  $k > 2\pi$ , but the latter is irrelevant here given that  $S_1(k, t)$  is typically very small for  $k > 2\pi$  after a very short ini-

tial time;  $S_1(k, t)$  was discussed by Lebowitz, Marro, and Kalos.<sup>6</sup>

The scaling behavior with time may be expressed as

$$S_1(k, t) = J_G(t)F(x), \quad x = kR_G(t), \quad t > t_s, \quad (4)$$

where  $R_G(t)$  is the scaling length obtained by following the Guinier method described in Ref. 3. Real and computer experiments<sup>3,6</sup> have shown that the scaling function  $F(x)$  decreases rather sharply for  $x > 1$  to a very small value [ $F(x) \approx 0$  in practice for  $x \geq 3$ ]. Also, as  $t$  increases,  $R_G(t) \rightarrow \text{const} \times L$  with  $L$  the linear dimension of the system. We thus expect that, by substitution of (3) and (4) in (2), one may write approximately after some initial regime

$$\frac{\Delta E(t)}{JN} = 12(1 - \rho - \rho_c)(\rho - \rho_c) \left[ 1 - \frac{J_G(t)}{R_G^3(t)} \int_0^\infty dx x^2 F(x) \right], \quad (5)$$

where  $\rho_c = (1 - \bar{\eta}_c)/2$ . The integral here normalizes to a constant,  $R_G^3(\infty)/J_G(\infty)$ , since  $\Delta E(t) \rightarrow 0$  as  $t \rightarrow \infty$ . Moreover, the ratio  $J_G(t)/R_G^3(t)$  is proportional<sup>3</sup> to the number of particles in the liquid phase,  $N[\rho - \rho(t)]$  where  $\rho(t)$  represents the density of the gas phase at time  $t$ , so that it follows that

$$\Delta E(t)/JN = 12(1 - \rho_c - \rho)[\rho(t) - \rho_c]. \quad (6)$$

This fundamental relation can be checked against Monte Carlo (MC) data; these support indeed a linear relation between  $E(t)$  and  $\rho(t)$  as shown by Fig. 1. Note that the prefactor in Eq. (6) is only roughly confirmed here because the data are very sensitive to our definition of liquid and gas phases in terms of the cut-off  $l_c$  (which should probably depend on temperature and density).

To exploit the consequences of Eq. (6) we may write the density  $\rho(t)$  of the gas phase in terms of a renormalized fugacity<sup>7</sup>  $w(t)$  such that

$$\rho(t) = \sum_{l=1}^{l_c} l w(t)^l Q_l (1 - \rho_c)^{k_l}.$$

Here  $Q_l$  represents a "cluster partition function"

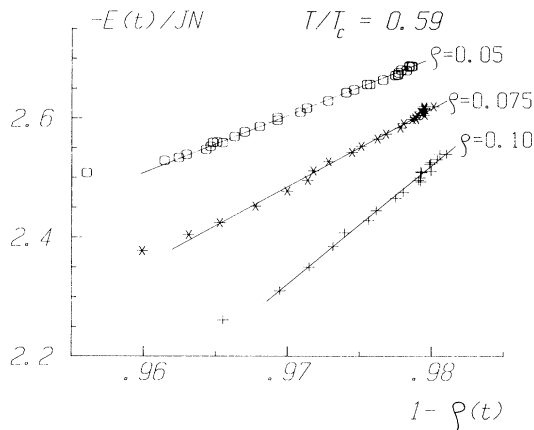


FIG. 1. The negative of the energy obtained in a MC computation as a function of the density of the gas phase ( $l \leq 10$ ) showing the linear dependence obtained in Eq. (6).

which only depends on  $l$  and  $T$ ,<sup>8</sup>  $k_1 = 3.25$ ,  $k_2 = 4.5$ ,  $k_3 = 5$ , and  $l \geq 3$ .  $\rho_c$  satisfies a similar equation with  $w(t)$  replaced by  $w_s$ , its equilibrium value. These two magnitudes can be related via the usual assumption  $w(t) = w_s[1 + f(\beta^{-1}t)]$ , with  $f(\beta^{-1}t) \rightarrow 0$  when  $t \rightarrow \infty$  and  $\beta$  depending on  $\rho$  and  $T$ . Reference 7 makes the extra assumption that  $f(\beta^{-1}t) \propto t^{-1/3}$  but this is not necessary here. We thus have

$$[w(t)/w_s]^l = [1 + f(\beta^{-1}t)]^l \approx 1 + lf(\beta^{-1}t)$$

and it follows that

$$E(t)/JN = \alpha f(\beta^{-1}t), \quad (7)$$

where  $\alpha$  and  $\beta$  are density- and temperature-dependent parameters. The scaling relation (7) is what was essentially observed in the microcalorimetric measurements reported before<sup>9</sup>; the above derivation thus provides a simple explanation of an interesting general behavior which seems well confirmed by experiments. This agreement also provides further indirect evidence for some assumptions involved in our discussion in this paragraph which are of interest in nucleation theory.<sup>7</sup>

In order to study deeply the above results, we shall analyze the relevance of two mechanisms<sup>10</sup> during the system temporal evolution. Phase separation is said to occur by *Smoluchowski coagulation* or *effective cluster diffusion*<sup>4</sup> when the clusters diffuse through the system, meet, and coalesce. *Ostwald ripening* or *monatomic diffusion*,<sup>11</sup> on the other hand, corresponds to the situation where clusters grow (or shrink) via single-atom processes, the growth being competitive in the sense that (in a steady-state condition) the largest clusters grow at the expense of the smaller ones. These mechanisms can be seen<sup>4,5</sup> to imply an approximate behavior  $\Delta E(t) \sim t^{-b}$  with characteristic exponents  $b = \frac{1}{6}$  and  $\frac{1}{3}$  respectively in three dimensions. Using  $b = \frac{1}{5}$ <sup>12</sup> instead of  $b = \frac{1}{6}$  would not modify our main conclusions in the following. Also, the consideration of hydrodynamic interaction leads to  $b = 1$  but, as one should expect, this is definitely inconsistent with the data here. Thus we shall simply write, assuming that

both mechanisms can occur simultaneously in the system,

$$\Delta E(t) = \gamma_1 t^{-1/3} + \gamma_2 t^{-1/6} \quad (8)$$

where  $\gamma_1$  and  $\gamma_2$  will eventually be allowed a simple dependence on time to account for the possibility that the two mechanisms may vary their relative importance with time;  $\gamma_1$  and  $\gamma_2$  are then expected to take on constant values for relatively small  $t$  and for very large  $t$ . Note that Eq. (8) shows an unsatisfactory behavior for  $t \rightarrow 0$  but this is rather irrelevant to our purpose here because the data always show untypical behavior during the very initial regime of the evolution as a result of finite temperature of homogenization, memory effects, etc.

The behavior of Eq. (8) is made explicit in Fig. 2 where the data come from a MC calculation and from some microcalorimetric measurements on alloys (see Ref. 9 for details). Figure 2 confirms our expectation about constant values for  $\gamma_1$  and  $\gamma_2$  when  $t$  is large enough and when  $t$  is small enough. It also shows a maximum corresponding to a rather sharp transition between initial and final regimes which seem respectively dominated by effective cluster diffusion and monatomic diffusion. Note however that there is no time regime in Fig. 2 where only one of the mechanisms occurs; this fact explains the usual failure<sup>10</sup> when one makes log-log plots looking for a single exponent to describe the whole or part of the temporal evolution. The same statement probably holds for

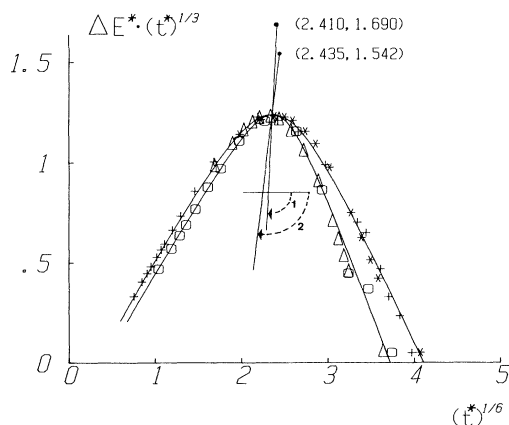


FIG. 2. The solid lines represent the two hyperbolas which correspond approximately to the two classes, deep and shallow quenches, with different dynamical behavior. The respective origins and principal axes are also shown; the angles denoted by 1 and 2 are respectively  $92.9^\circ$  and  $96.5^\circ$ . The data and corresponding scaling factors are as follows: MC data at  $0.59T_c$  and  $\rho = 0.20$  (crosses,  $\alpha = 1$ ,  $\beta = 1$ ), MC data at  $0.59T_c$  and  $\rho = 0.10$  (circles,  $\alpha = 2.597$ ,  $\beta = 0.567$ ), Al-Zn alloy at  $0.59T_c$ , 6.8 at.% (triangles,  $\alpha = 187$  J/mol,  $\beta = 312$  s), Al-Zn alloy at  $0.59T_c$ , 10 at.% (asterisks,  $\alpha = 266$  J/mol,  $\beta = 119$  s).

other quantities such as the moments of the structure function or cluster distribution. The shape of the curve in Fig. 2 also seems in contradiction with the speculation of Furukawa<sup>12</sup> that various growth mechanisms occur intermittently.

The plot in Fig. 2 is also convenient to demonstrate the kind of scaling derived before, Eq. (7), and to analyze some other open questions. As a matter of fact, a similar plot in Ref. 9 seems to indicate that the phase points inside the coexistence curve for the lattice model described before and for a number of aluminum alloys can be grouped into two different classes, corresponding to different shapes of the curve in Fig. 2, showing differences in their system dynamics. In order to be able to elucidate this important point (by stimulating new microcalorimetric studies) we propose a graphical method which should also provide clear evidence for the properties (7) and (8).

The method requires a set of data as an (arbitrary) reference; let us take for this purpose the data obtained by MC calculations applied to the lattice model evolving at  $T/T_c = 0.59$  with  $\rho = 0.20$ . These data, when plotted as in Fig. 2, show a maximum at  $X_m = 2.33 \pm 0.03$ ,  $Y_m = 1.24 \pm 0.02$  in the (nondimensional) MC units and can be fitted quite well by the hyperbola  $X^2/C_1^2 + Y^2/C_2^2 = 1$  with  $C_1 = 0.450$ ,  $C_2 = 0.521$ , the origin at  $(2.410, 1.690)$ , and the axis rotated  $-92.9^\circ$ . We believe that, in analogy with the situation in Ref. 6 where the data corresponding to the structure function are analyzed, this curve is representative of a class of phase points with similar dynamical behavior which will be termed *deep quenches*. In contrast, *shallow quenches*, which can be represented, for instance, by the MC data at  $T/T_c = 0.59$  and  $\rho = 0.10$ , seem to behave slightly differently, namely, they are fitted instead by a hyperbola with  $C_1 = 0.306$ ,  $C_2 = 0.328$ , the origin at  $(2.435, 1.542)$  and the axis rotated an angle  $-96.5^\circ$ ; see Fig. 2.

Any experimental data concerning measurements of the excess energy can thus be compared with those hyperbolas in order to analyze the range of validity of the above results, particularly (7) and (8), and whether one can indeed distinguish between deep and shallow quenches, a question related to the problem of metastability. To this end one may make a plot of the experimental data in terms of the reduced variables  $E^* = \alpha^{-1}E$  and  $t^* = \beta^{-1}t$ , where  $\alpha$  and  $\beta$  are scaling parameters (dependent on  $T$  and  $\rho$ ) such that the curve  $\Delta E^*(t^*)^{1/3}$  versus  $(t^*)^{1/6}$  has its maximum at  $(X_m, Y_m)$ . Figure 2 includes two examples which show the typical order of magnitude of the scaling parameters  $\alpha$  and  $\beta$ . Note that Fig. 2 is indeed strong evidence in favor of the simultaneous occurrence of both mechanisms of evolution, effective cluster diffusion being initially dominant while monatomic diffusion seems to play the most important role during the final

regime  $t^* \geq 160 \pm 20$ , and in favor of the scaling *Ansatz* (7) with a "universal" function  $f$ . The function  $f$  can be represented (excluding very small  $t$ ) as in Eq. (8), or by the mentioned hyperbolas, and it seems to be slightly different for deep than for shallow quenches.

Finally, we wish to mention that our results are also consistent with previous findings. The ordinate of the maximum in Fig. 2, i.e., the time  $t^* \simeq 160$  separating, say, Smoluchowski coagulation from Ostwald ripening type of evolution, is consistent with the time  $t_C$  estimated in Ref. 13 for the changeover from Cahn-Hilliard-Cook behavior to more complex, nonlinear behavior. Moreover, our distinction between deep and shallow quenches is also inferred in Ref. 6 from different data and point of view, and can be seen to be roughly consistent with crude mean-field criteria.<sup>14</sup>

This work was supported by the Comisión Asesora de Investigación Científica y Técnica, Spain.

Sahni, in *Phase Transitions and Critical Phenomena*, edited by C. Domb and J. L. Lebowitz (Academic, New York, 1983), Vol. 8.

<sup>2</sup>J. Marro, J. Lebowitz, and M. Kalos, *Phys. Rev. Lett.* **43**, 282 (1979).

<sup>3</sup>P. Fratzl, J. L. Lebowitz, J. Marro, and M. Kalos, *Acta Metall.* **31**, 1849 (1983).

<sup>4</sup>K. Binder and D. Stauffer, *Phys. Rev. Lett.* **33**, 1006 (1974).

<sup>5</sup>K. Binder, *Phys. Rev. B* **15**, 4425 (1977).

<sup>6</sup>J. Lebowitz, J. Marro, and M. Kalos, *Acta Metall.* **30**, 297 (1982).

<sup>7</sup>O. Penrose, J. Lebowitz, J. Marro, M. Kalos, and A. Sur, *J. Stat. Phys.* **19**, 243 (1978).

<sup>8</sup>J. Marro and R. Toral, *Physica (Utrecht)* **122A**, 563 (1983).

<sup>9</sup>J. Marro, R. Toral, and A. M. Zahra, *J. Phys. C* (to be published).

<sup>10</sup>K. Binder, M. Kalos, J. Lebowitz, and J. Marro, *Adv. Colloid Interface Sci.* **10**, 173 (1979).

<sup>11</sup>I. M. Lifshitz and V. V. Slyozov, *J. Phys. Chem. Solids* **19**, 35 (1961); C. Wagner, *Z. Elektrochem.* **65**, 58 (1961).

<sup>12</sup>H. Furukawa, to be published.

<sup>13</sup>J. Marro and J. L. Vallés, *Phys. Lett.* **95A**, 443 (1983).

<sup>14</sup>K. Binder, *Phys. Rev. A* **29**, 341 (1984).

---

<sup>1</sup>See, for instance, J. D. Gunton, M. San Miguel, and P. S.